JOURNAL OF BACTERIOLOGY, Apr. 2006, p. 2959–2973 Vol. 188, No. 8
0021-9193/06/$08.00+0 doi:10.1128/JB.188.8.2959–2973.2006

Transcription of the Contiguous *sigB*, *dtxR*, and *galE* Genes in *Corynebacterium diphtheriae*: Evidence for Multiple Transcripts and Regulation by Environmental Factors

Diana Marra Oram,† Andrew D. Jacobson, and Randall K. Holmes*

Department of Microbiology, University of Colorado School of Medicine, Aurora, Colorado 80045

Received 4 November 2005/Accepted 7 February 2006

The iron-dependent transcriptional regulator DtxR from *Corynebacterium diphtheriae* is the prototype for a family of metal-dependent regulators found in diverse bacterial species. The structure of DtxR and its action as a repressor have been extensively characterized, but little is known about expression of *dtxR*. In the current study, we investigated transcription of *dtxR* as well as the *sigB* and *galE* genes located immediately upstream and downstream from *dtxR*, respectively. We identified two promoters that determine transcription of *dtxR*. The first, located upstream of *sigB*, appears to be controlled by an extracytoplasmic function σ factor. The second, located in the intergenic region between *sigB* and *dtxR*, is similar to promoters used by the primary vegetative σ factors in other actinomycete species. Using quantitative real-time assays, we demonstrated that the number of transcripts initiated upstream from *sigB* is affected by several environmental factors. In contrast, the presence of sodium dodecyl sulfate was the only factor tested that conclusively affects the number of transcripts initiated in the *sigB-dtxR* intergenic region. Additionally, we provided evidence for the existence of transcripts that contain *sigB*, *dtxR*, and *galE*. Our studies provide the first quantitative transcriptional analysis of a gene encoding a DtxR family regulator and give new insights into transcriptional regulation in *C. diphtheriae*.

Transcriptional regulators in the diphtheria toxin repressor (DtxR) family control gene expression in response to changes in the concentration of iron and/or manganese in a wide variety of bacterial species (2, 3, 16, 19, 21, 25, 54, 55). DtxR-like proteins are the predominant iron-dependent regulators in many acid-fast and gram-positive species, whereas the ferric uptake regulator (Fur) is the primary iron-dependent regulator in most gram-negative bacteria (18a). DtxR, the prototype of the family, is best characterized as a regulator that controls transcription of *tox*, the gene encoding diphtheria toxin in lysogenic strains of *Corynebacterium diphtheriae* (22). In its dimeric iron-bound form, holo-DtxR binds to an operator sequence within the *tox* promoter and prevents transcription of *tox*. In the apo form without bound iron, DtxR is unable to bind its cognate operator sequence, repression is relieved, and transcription of *tox* proceeds. In addition to controlling expression of *tox*, holo-DtxR represses transcription of several other genes, most of which are involved in iron uptake and utilization (27, 28, 43, 50, 56). In *Mycobacterium* species, the DtxR homologue IdeR acts to repress transcription of some genes involved in iron homeostasis and to activate transcription of others (9, 15, 46). The gene encoding DtxR can be inactivated in *C. diphtheriae*, but the resulting strain has a significant growth defect and is more sensitive to oxidative stress than its wild-type parent (40). Inactivating the gene encoding IdeR in *Mycobacterium smegmatis* causes a similar phenotype of increased sensitivity to oxidative stress (8), but in *Mycobacterium tuberculosis ideR* is essential for viability (47). Clearly, DtxR-like proteins are versatile transcriptional regulators that are often required for vital cellular functions.

The DNA binding activity, metal specificity, and physical structure of DtxR have been well characterized. DtxR binds as a dimer to palindromic 19-bp DNA operator sequences within the promoters of the genes that it regulates (51, 59, 60). Transcriptional regulation by DtxR in vivo is observed in response to changing iron concentrations, but sequence-specific binding of DtxR to DNA in vitro can be activated by other divalent transition metals, including cadmium, cobalt, manganese, nickel, and zinc (51, 53, 59). Extensive crystallographic studies have shown that DtxR has three domains (12, 45, 49). Amino acids 1 to 73 form domain 1, which contains a classical helix-turn-helix DNA-binding motif. Domain 2 (amino acids 74 to 140) determines dimerization of DtxR and contains the binding sites for two Fe^{2+} ions per monomer. The final 86 amino acids of DtxR (residues 141 to 226) comprise domain 3, which contributes ligands to one of the metal binding sites and has topology similar to the SH3 domains found in some eukaryotic signal transduction proteins (44). The first two domains of DtxR are essential for DtxR to function as a transcriptional repressor, while domain 3 is thought to modulate the activity of DtxR at individual promoters (30, 41).

While much research has focused on characterizing the structure and function of DtxR as a transcriptional regulator, little is known about the expression of *dtxR*. Analysis of RNA isolated from *C. diphtheriae* showed that the abundance of *dtxR* transcripts is much less than the abundance of *tox* transcripts under low-iron conditions, and the prevalence of *dtxR* transcripts is not affected by the amount of iron in the growth medium (52). This correlates well with the observation that the levels of DtxR in *C. diphtheriae* are not influenced by available

* Corresponding author. Mailing address: University of Colorado at Denver and Health Sciences Center, School of Medicine, Department of Microbiology, Mail Stop 8333, P.O. Box 6511, Aurora, CO 80045. Phone: (303) 724-4224. Fax: (303) 724-4226. E-mail: Randall.Holmes@uchsc.edu.

† Present address: University of Maryland Dental School, Department of Biomedical Sciences, Baltimore, MD 21201.

iron (40). Quantitative analysis shows that *C. diphtheriae* contains approximately 750 dimers of DtxR per cell under both high- and low-iron conditions (39). The *C. diphtheriae* genome sequence reveals that *dtxR* is located 224 bp downstream from *sigB*, which is predicted to encode a sigma factor with homology to σ^{70}-type factors, and 22 bp upstream from *galE*, which is predicted to encode a UDP-galactose 4-epimerase (4). Previously we reported preliminary evidence indicating that *sigB* and *dtxR* as well as *dtxR* and *galE* are cotranscribed (40).

The genetic organization of *sigB* and *dtxR* in *C. diphtheriae* is very similar to that in several other actinomycete species including *M. tuberculosis* (6) and *Brevibacterium lactofermentum* (37). In *M. tuberculosis*, *B. lactofermentum*, and *Brevibacterium flavum*, *sigB* is transcribed from a promoter located approximately 25 bp upstream from the coding sequence, and several environmental stress conditions have been shown to affect expression of *sigB* in these species (17, 23, 37, 38). In addition, in *C. diphtheriae* and *B. lactofermentum*, a *galE* homologue is located immediately downstream from *dtxR*. The transcripts encoding all three genes in this locus were examined in *B. lactofermentum*, using Northern blot assays. Two *sigB*-containing transcripts were identified; one includes only *sigB* and the other contains *sigB* as well as a portion of the *dtxR* homologue *dmdR*. Similarly, the complete *dmdR* gene is encoded on two different transcripts: one contains only *dmdR* and the other includes both *dmdR* and *galE* (36).

Although the activity of DtxR has been studied by many researchers, the transcription of *dtxR* and contiguous genes has not been investigated in *C. diphtheriae*. In the present study, we investigated the transcriptional regulation of the genes in the *dtxR* locus with the goals of understanding better the mechanisms of transcriptional regulation in *C. diphtheriae* and the role of DtxR in the pathogenesis of diphtheria. We showed that the promoter located upstream from *sigB* functions in *C. diphtheriae* but not in *Escherichia coli*, clearly indicating a role for species-specific factors in the regulation of transcription in *C. diphtheriae*. Furthermore, we demonstrated that transcription at the *dtxR* locus is affected by environmental factors and that *dtxR* can be cotranscribed with the genes that surround it. Transcription of *dtxR* is a complex and multifaceted process that is controlled both by DNA regulatory elements that exert their effects in *cis* and by soluble regulatory factors that exert their effects in *trans*.

MATERIALS AND METHODS

Bacterial strains and cultivation conditions. The toxigenic *C. diphtheriae* strain C7(β) (1) was isolated after β phage infection of strain C7(−) (13) and has been used extensively for experimental work since the 1950s. *E. coli* DH5α (Bethesda Research Laboratories, Gaithersburg, Md.) was used as a host for cloning and β-galactosidase assays. *C. diphtheriae* strains were cultivated in PGT, which is a deferrated casein hydrolysate medium (1) or heart infusion broth (BD-Difco, Franklin Lakes, NJ) supplemented with 0.2% Tween 20 (HIBTW). *E. coli* strains were cultivated in Luria-Bertani broth (33). Kanamycin was added at a concentration of 20 μg/ml and spectinomycin was added at a concentration of 100 μg/ml for *C. diphtheriae*. Ampicillin was added at a concentration of 100 μg/ml for *E. coli*. Medium was deferrated by adding 15 g/liter Chelex-100 (Bio-Rad, Hercules, CA) and mixing it for 2 h followed by filter sterilization.

Construction of Δ*dtxR*. First, to eliminate PstI sites in the vector portion of the *dtxR*-containing plasmid pMS297, the 1,533-bp EcoRI-to-BamHI fragment which contains *dtxR* (54) was ligated to pBluescript II KS (Stratagene, La Jolla, CA) digested with EcoRI and BamHI to construct pMS297.1. Next pMS297.1 was used as a template in PCR with the primers M13-20 and dtxR1CBE to generate a 671-bp product with a unique PstI recognition site introduced by the primer dtxR1CBE as well as the site for BamHI. The PCR fragment was digested with PstI and BamHI and ligated to the 3,635-bp PstI-to-BamHI fragment of pMS297.1 to construct pCB300. The plasmid pCB300 contains a deletion within *dtxR*, but the reading frame is shifted +1 from the original *dtxR* reading frame. To return the gene to its original reading frame, pCB300 was digested with PstI followed by treatment with T4 DNA polymerase to remove the 3′ single-stranded nucleotide overhangs, resulting in the deletion of 4 bp. The molecule was religated to construct pCB300IN, and DNA sequencing was used to confirm the expected DNA sequence within the region encoding the deleted form of *dtxR*. The plasmid pCB300IN contains a deletion within *dtxR* that maintains the original reading frame. The restriction enzymes EcoRI and XbaI were used to digest pCB300IN, and the 1,284-bp fragment containing the deleted version of *dtxR* was ligated to the identically digested vector pK19mobsacB (48) to produce pCB301IN. The plasmid pCB301IN contains an RP4 origin of transfer and was transformed into RP4-mobilizing *E. coli* S17-1 (58).

Mating of *E. coli* and *C. diphtheriae* was performed as described in reference 61 with slight modifications. S17-1/pCB303IN and *C. diphtheriae* C7(β) were grown overnight, and the cultures were concentrated 10-fold in sterile medium. One-hundred-microliter aliquots of each concentrated sample were spread together on heart infusion agar plates and incubated at 30°C for 16 h. Corynebacterial cointegrates were isolated by plating bacteria scraped from the conjugation plate on heart infusion agar plates supplemented with 30 μg/ml nalidixic acid and 10 μg/ml kanamycin. To resolve the cointegrates, single kanamycin-resistant colonies were picked and grown overnight at 37°C in PGT plus 50 μg/ml ethylenediamine-*N*,*N*-diacetic acid (EDDA), and then 100 μl of the overnight culture was plated on heart infusion agar plus 15% sucrose and 10 μg/ml EDDA. The agar plates were incubated at 37°C overnight, and sucrose-resistant colonies were screened for sensitivity to kanamycin (to confirm loss of the integrated plasmid). Finally, the primers dtxRcr1 and dtxRA3 were used in PCR to screen for the subset of colonies in which loss of the integrated plasmid was accompanied by substitution of a deleted copy of *dtxR* for the wild-type *dtxR* allele in the chromosome. The nucleotide sequence of the deleted copy of *dtxR* (Δ*dtxR*) in the chromosome of C7(β) was confirmed by DNA sequencing.

Growth rate determinations. The growth rates for selected strains of *C. diphtheriae* were determined in PGT medium, PGT medium plus 10 mM $FeCl_3$, and HIBTW medium. Strains were inoculated to an absorbance at 600 nm (A_{600}) of approximately 0.1. The cultures were incubated at 37°C with shaking, and the A_{600} was monitored for 8 to 15 h or until the cells entered stationary phase. The growth rate of each strain during log phase was determined and compared to that of wild-type C7(β).

Measurement of diphtheria toxin and siderophore. Diphtheria toxin in the supernatant of cultures was determined by using the enzyme-linked immunosorbent assay described previously (40). Siderophore was detected in culture supernatants using a slightly modified version of the CAS assay described previously (40). The CAS assay was adapted so that reactions could be performed in 96-well microtiter plates by altering the total volume of each sample from 1 ml to 0.2 ml. The absorbances of the reaction mixtures were then read in a microplate reader at a wavelength of 630 nm.

Resistance to killing by hydrogen peroxide. Resistance to killing by hydrogen peroxide, H_2O_2, was assayed as described previously (40). Briefly, in the zone of inhibition assay we measured the diameters of the zones of inhibition of bacterial growth produced when 20 μl of 1 M H_2O_2 was applied to 0.6-cm-diameter paper disks in the centers of plates containing heart infusion agar and lawns of various strains of *C. diphtheriae*.

In the percent killing assay cultures were grown in PGT until the absorbance of the culture measured at 600 nm was between 0.5 and 0.8, at which time H_2O_2 was added to the growth medium at a final concentration of 50 mM and the cultures were then incubated for an additional 30 min. Viable counts from each culture were then determined by plating dilutions of the culture onto heart infusion agar.

Construction of reporter plasmids and β-galactosidase assays. The expression vector pSPZ that was used to determine β-galactosidase activity encoded by a *lacZ* reporter gene in *C. diphtheriae* was constructed by ligating the 1.2-kb FspI-to-NsiI fragment of pJKS1 (40) to the 7.7-kb NsiI to NruI fragment of pKMZ (Y. Qian and R. K. Holmes, unpublished data). This fragment of pKMZ contained transcriptional terminators and the promoterless *lacZ* gene from pCM502 (50) as well as the stable replication origin of pNG2 (57). The plasmid pSPZ encodes resistance to spectinomycin. To construct the promoter fusion plasmids used in Fig. 4, the following DNA fragments were cloned into either pSPZ (for assays in *C. diphtheriae*) or pQF50 (for assays in *E. coli*): dtxRUP, generated by PCR amplifying a region containing the 5′ end of *dtxR* and a portion of *sigB* with the primers dtxRPE1 and dtxRH3 (the sequences of all primers are shown in

TABLE 1. Primers and probes

Name	Sequence, 5′ to 3′	Binding site and/or purpose	Reference or source[a]
Primers for cloning, screening, and primer extension			
dtxR1	TAAAGCGCATGCTTAGATATGCC	Upstream of *dtxR*, cloning	*
dtxR2	CTAGCATGCAACAAGAAAACG	Upstream of *dtxR*, cloning	*
dtxRA3	CAGACACTTCCTACGTATCCGGC	Downstream of *dtxR*, RT-PCR	*
dtxR1CBE	GCCTGCAGCGCAAAGTACGC	3′ end of *dtxR*, cloning	*
dtxRcr1	GTCGATACCACCGAGATGTA	5′ end of *dtxR*, RT-PCR	39
dtxRH3	GAGCAGGTAAACAAGCTTTCTCG	Middle of *sigB*, cloning (A, Fig. 1)	*
dtxRPE1	GCAAGTAAAGCTTTGTGGTATCG	5′ end of *dtxR*, cloning	*
dtxRPE2	CCTTATAGTGCCATGGAGACTG	Upstream of *dtxR*, primer extension	*
kntsprev	GGTGATCAATTCCTATCAATC	Upstream of *dtxR*, primer extension	*
lacZ2	GGAAGCAGCCCAGTAGTAGGTTG	Near polylinker in pSPZ and pQF50, cloning	*
M13-20	GTAAAACGACGGCCAGT	pBluscript vectors, cloning	New England Biolabs (Beverly, MA)
MCS3	AACTCGGCGTAGGCAATT	3′ end of *dtxR*, cloning	*
MS5	AGAACAGTCGACCAGACACTTCCTA	5′ end of *galE*, cloning	*
Qflac	CGGCCAGTGAATCCGAATTCCCTTTC	Near polylinker in pSPZ and pQF50, cloning	*
sigBPE3	CCGCGGTCGACGGTCTCCGTGG	5′ end of *sigB*, primer extension	*
sigBPEBam	GTGGATGGATCCACGTCGGAAGGGC	5′ end of *sigB*, cloning	*
sigBXhoI	CGGACTGCGATCTCGAGGAAT	Upstream of *sigB*, cloning	*
Primers and probes for qPCR			
dtxR-Afor	CGTCAATTTGGACTGTCTCG	3′ end of *sigB* (B, Fig. 1)	*
dtxR-Arev	AAGCAAACGCTTTATTGTGC	3′ end of *sigB* (d, Fig. 1)	*
dtxR-Aprobe	AGAGTTCGCCAAATTGAACG	3′ end of *sigB* (SB, Fig. 1)	*
dtxR-Bfor	CCAGCACACAACAGTCTCCA	5′ end of *dtxR* (C, Fig. 1)	*
dtxR-Brev	CAGATTGTTCCAGACGCTCA	5′ end of *dtxR* (c, Fig. 1)	*
dtxR-Bprobe	CTCTTCGCGCTAGGATCG	5′ end of *dtxR* (DR, Fig. 1)	*
galE1for	CACACTATTCGTATCGAAGAACTC	3′ end of *dtxR* (F, Fig. 1)	*
galE1rev	GGAACAGACACTTCCTACGTATCC	5′ end of *galE* (b, Fig. 1)	*
galE1probe	AGGCGGCGAAATTAGATGAAAC	Intergenic region between *dtxR* and *galE* (DG, Fig. 1)	*
galE2for	CATACGGCGAACCCGAAACAGTCCCG	5′ end of *galE* (G, Fig. 1)	*
galE2rev	CGCAGCAAACCCATATGCATGTGC	5′ end of *galE* (a, Fig. 1)	*
galE2probe	CTGAAGACGCTCCTACCCAC	5′ end of *galE* (GE, Fig. 1)	*
sigA RTF	GATGAATTTGACGACGACGA	*sigA*	*
sigA RTR	GAAAGCTCCGCATCTTTACG	*sigA*	*
sigA RTP	CGGAGAAGATGACTCTTCCG	*sigA*	*
toxBF-RT	CGCCCTAAATCTCCTGTTTATGTT	*tox*	34
toxBR-RT	GTACCCAAGAACGCCTATGGAA	*tox*	34
toxB probe	TTCACAGAAGCAGCTCGGAGAAAA TTCATTC	*tox*	34

[a] *, this work.

Table 1); dtxRU1, generated by PCR amplifying the region upstream of *dtxR* with the primers dtxR1 and dtxRPE1; dtxRU2, the portion of dtxRU1 downstream of the NcoI recognition site; dtxRU3, the portion of dtxRU1 upstream of the NcoI recognition site; dtxRU4, generated by PCR amplifying the region upstream of *dtxR* with the primers dtxR2 and dtxRPE1; sigBUP, generated by amplifying the region upstream of *sigB* with the primers sigBPEBam and sigBX hoI; and galEUP, generated by amplifying the region upstream of *galE* with the primers MCS3 and MS5. To ensure that no nucleotide changes had been introduced during cloning and PCR amplification, DNA sequencing was used to confirm the correct sequence of each fragment.

In *E. coli*, promoter activity was measured in low-iron medium consisting of deferrated Luria-Bertani medium plus 100 μM each of $MgCl_2$, $MnCl_2$, $ZnCl_2$, and $CaCl_2$ and in high-iron medium consisting of low-iron medium plus 10 μM $FeCl_3$. In *C. diphtheriae*, promoter activity was measured in low-iron medium consisting of deferrated PGT and high-iron medium consisting of PGT plus 10 μM $FeCl_3$. Assays were performed on three overnight cultures on a single day, and independent experiments were performed on at least three different days. Units of β-galactosidase activity were determined using the method of Miller (33) in *E. coli*, and in *C. diphtheriae* the Miller method was altered slightly by increasing the concentration of sodium dodecyl sulfate (SDS) by 100-fold to permeabilize the cells.

Isolation of RNA. *C. diphtheriae* cultures were pelleted by centrifugation and resuspended in acidified phenol (pH 4.3). The samples were then transferred to screw-cap tubes containing 0.1-mm glass beads and diethyl pyrocarbonate-treated water. Each tube was processed in a Minibeater (BioSpec, Bartlesville, OK) for 1 min at 4°C at full speed. The bead-beating process was repeated three times with the samples being placed on ice for 1 min between bead-beater cycles. Samples were next spun in a microcentrifuge at full speed for 8 min, and the top phase was removed to a new tube. The samples were extracted three times with equal volumes of acidified phenol and chloroform. The RNA was precipitated with 3 volumes of 95% ethanol and 0.1 volume of 3 M sodium acetate, pH 4.8. After being washed with 75% ethanol, the RNA was resuspended in diethyl pyrocarbonate-treated water and treated with RQ1 DNase (Promega, Madison, WI) per the manufacturer's instructions for 4 h at 37°C. Following DNase treatment the RNA was once again ethanol precipitated as described above.

RNase protection and primer extension assays. RNase protection assays were performed using the RPAIII RNase protection kit (Ambion, Austin, TX) per the manufacturer's instructions. The gene-specific probes for *dtxR* consisted of sin-

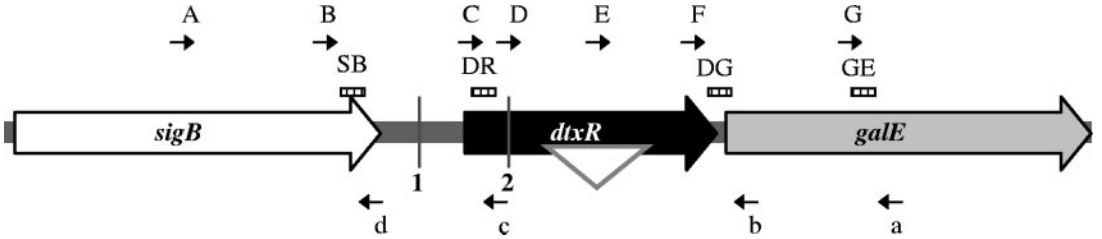

FIG. 1. The region of the *C. diphtheriae* C7(β) chromosome that includes *sigB*, *dtxR*, and *galE* is depicted. The region of *dtxR* deleted in the Δ*dtxR* strain is shown as a white inverted triangle within *dtxR*. The locations of the transposon insertions in C7(β)*dtxR*-TnUP labeled as 1 and in C7(β)*dtxR*-TnIN labeled as 2 are shown as vertical gray lines. The positions of primer binding sites are shown as small black arrows labeled A, B, C, D, E, F, G, a, b, c, and d. The fluorescent probes used in qRT-PCR assays are shown as striped rectangles labeled SB, DR, DG, and GE. The sequences of the primers and probes are given in Table 1.

gle-stranded RNA generated in vitro using T7 RNA polymerase (Fermentas, Hanover, MD) per the manufacturer's protocol. The construction of the plasmids used as templates in the transcription reaction is described below. To construct pBSdtxR1, the 1,400-bp PCR product containing *dtxR*, generated in PCR with the primers dtxRH3 and dtxRA3, was digested with HindIII and AgeI and ligated to pBluescript II KS (Stratagene, La Jolla, CA) digested with HindIII and XmaI. All plasmids used as transcription templates were derived from pBSdtxR1. To construct pBSdtxR1-1, pBSdtxR1 was digested with BamHI and Tth111I; to construct pBSdtxR1-2, pBSdtxR1 was digested with BamHI and NcoI; and finally to construct pBSdtxR1-3, pBSdtxR1 was digested with BamHI and PstI. The ends of the resulting linear DNA fragments were blunted using T4 DNA polymerase, and each fragment was circularized with T4 ligase to construct the corresponding plasmid. The plasmid pBSdtxR1-3 was digested with NcoI and used as a template in the in vitro transcription reaction with [^{32}P]CTP to generate probe 1 (shown in Fig. 5). The plasmid pBSdtxR1-1 was digested with *Xmn*I and used to generate probe 2, and the plasmid pBSdtxR1-2 was digested with PvuII and used to generate probe 3. Each probe contains a portion of the *dtxR* sequence as shown in Fig. 5 as well as a 5′ end identical to the polylinker region of the pBluescript II KS vector. Each ^{32}P-labeled probe was purified on a 6% denaturing acrylamide gel before it was used in the RNase protection assay.

Primers used in the primer extension assays were labeled with [^{32}P]ATP using T4 polynucleotide kinase (Fermentas) per the manufacturer's protocol. Each primer was purified away from unincorporated nucleotide using a G25 Sepharose spin column. The labeled primers were used in both the sequencing and the primer extension reactions. Sequencing was performed using the fmol DNA cycle sequencing system (Promega, Madison, WI) per the manufacturer's instructions. The primer extension reactions were performed with Superscript III reverse transcriptase (Invitrogen, Carlsbad, CA) per the manufacturer's protocol. Sequencing reactions and primer extension reactions were run on a 6% acrylamide urea denaturing gel as shown in Fig. 5 and 6.

Generation and detection of cDNA. To generate cDNA, 1 μg of total RNA was used as a template in reaction mixtures containing a primer specific for the gene of interest and Superscript III reverse transcriptase (Invitrogen). The reaction conditions were as recommended by the manufacturer in a total volume of 20 μl. The cDNA was detected using PCR. For standard PCR, 5 μl of the reverse transcriptase reaction product was used as a template with gene-specific primers and *Taq* DNA polymerase. Reactions were performed using standard PCR conditions in a thermocycler.

For real-time quantitative reverse transcriptase PCR (qRT-PCR) 1 μl of the reverse transcriptase reaction product was used as a template in reactions using Cepheid Omnimix beads, primers specific for the gene of interest, and a probe synthesized by Integrated DNA Technologies, Coralville, IA, that included 5′ 6-carboxyfluorescein and 3′ black hole quencher 1 modifications. The final reaction volume was 25 μl. Reactions were performed in a Cepheid Smartcycler II using the following conditions: 75°C for 75 s and then 50 cycles of 95°C for 5 s and 59°C for 40 s. Fluorescence was monitored and recorded. DNA containing the gene of interest was used to generate a standard curve for each probe using these conditions. The primers and probes used to detect transcripts containing the gene of interest are listed in Table 1.

Stress conditions. *C. diphtheriae* cultures were grown in low-iron PGT medium until the absorbance at 600 nm was 4 to 5, at which point the cultures were exposed to the particular stress for 35 min. For acid stress, the pH of the medium was adjusted to 4.5 with HCl; for cold stress, the cultures were shifted to 15°C; for ethanol stress, a final concentration of 5% ethanol was added; for H_2O_2 stress, a final concentration of 10 mM hydrogen peroxide was added; for heat stress, the cultures were shifted to 45°C; for salt stress, a final concentration of 2.5% NaCl was added; and for SDS stress, a final concentration of 0.05% sodium dodecyl sulfate was added. Following exposure to each stress condition, the cells were pelleted and RNA was harvested as described above.

RESULTS

Construction of C7(β)Δ*dtxR*. Previously, we identified two transposon mutants of *C. diphtheriae* C7(β), designated C7(β)18.5 and C7(β)3B11, both of which show altered expression of *dtxR* (40). C7(β)3B11 (hereafter referred to as the *dtxR*-TnUP strain) has a transposon inserted 121 bp upstream of the *dtxR* ATG start codon and produces threefold-less DtxR than C7(β) does. C7(β)18.5 (hereafter referred to as the *dtxR*-TnIN strain) has a transposon inserted within *dtxR* (Fig. 1) and fails to produce any detectable DtxR. To eliminate possible phenotypic consequences of polar effects caused by these transposon insertions, we constructed C7(β)Δ*dtxR*, which has an in-frame deletion from bp 220 to bp 481 within *dtxR* (bp 1 is the A of the ATG start codon). This deletion removes the coding sequence for 87 amino acids from Ala74 through Pro160, corresponding to all of domain 2 and part of domain 3. Western blots of extracts from C7(β)Δ*dtxR* and C7(β)*dtxR*-TnIN using polyclonal anti-DtxR144+ (41) showed no immunoreactive DtxR, but DtxR was easily detected in Western blots with extracts from wild-type C7(β) and C7(β)*dtxR*-TnUP (data not shown).

Phenotypes of *dtxR* mutant strains. We compared wild-type C7(β) with the *dtxR* transposon insertion and internal-deletion mutants with respect to growth rate, iron regulation of diphtheria toxin and siderophore production, and susceptibility to H_2O_2. The growth rates were determined in three different media: HIBTW, PGT, and PGT supplemented with 10 μM $FeCl_3$ (for components of each medium see Materials and Methods). The doubling times of the mutants in each medium were normalized to the doubling time of C7(β) in the same medium. C7(β)*dtxR*-TnUP had a doubling time of 1.1 to 1.3 times that of C7(β), whereas C7(β)*dtxR*-TnIN and C7(β)Δ*dtxR* had normalized doubling times of 1.2 to 1.5 times that of C7(β). In each medium, C7(β) had the shortest doubling time, and C7(β)*dtxR*-TnUP grew faster than C7(β)*dtxR*-TnIN and C7(β)Δ*dtxR*. In PGT plus 10 μM $FeCl_3$, the differences among strains were greatest and C7(β)dtxR-TnIN and C7(β)Δ*dtxR* exhibited their longest doubling times of 80 to 90 min [1.5 times that of C7(β)]. Following transformation with pJKSdtxR, which determines production of approximately five times the

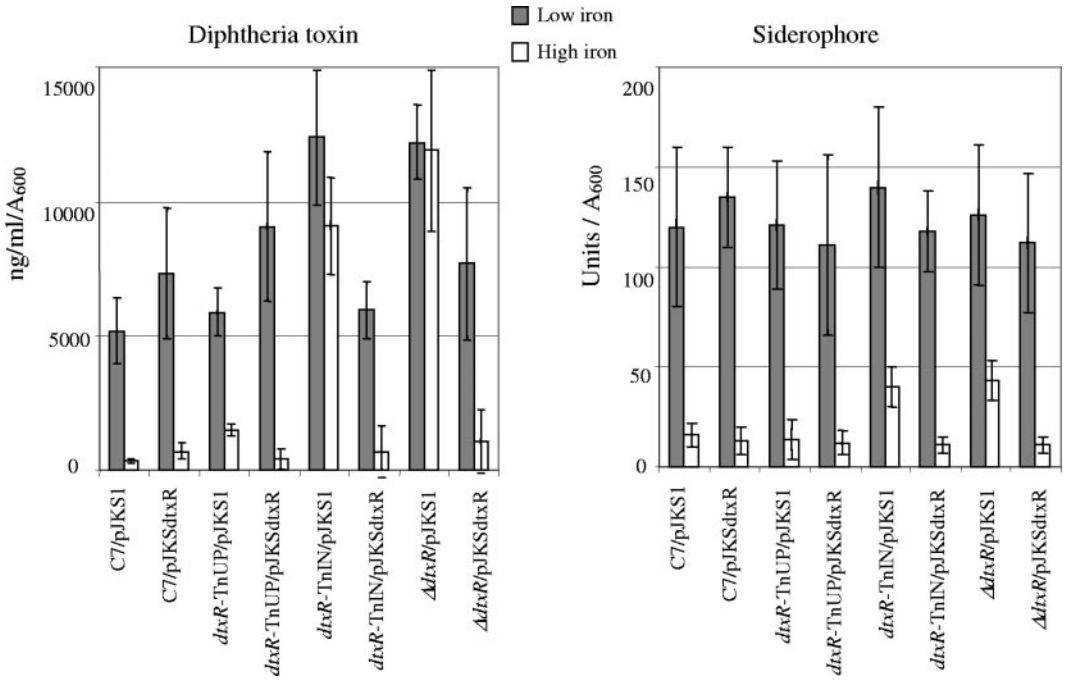

FIG. 2. The ability of each strain to repress diphtheria toxin production in the presence of iron is shown on the left. The nanograms of diphtheria toxin detected in an ELISA per milliliter of culture per absorbance of the culture at a wavelength of 600 nm is indicated. The ability of each strain to repress production of siderophore in the presence of iron is shown on the right. Siderophore units detected in a CAS assay per absorbance of the culture at a wavelength of 600 nm are indicated. All strains are lysogens of corynebacteriophage β. In both charts the error bars indicate the standard deviations of the values from three independent cultures subjected to the appropriate assay.

amount of DtxR found in C7(β) (40), the growth rate for all mutant strains was comparable to that of C7(β).

Next, we examined the regulation of diphtheria toxin and siderophore production by iron (Fig. 2). Under high-iron conditions, C7(β)Δ*dtxR* and C7(β)*dtxR*-TnIN failed to repress production of diphtheria toxin, whereas C7(β)*dtxR*-TnUP showed a slight defect in repression compared with C7(β). The amounts of toxin produced under low-iron conditions were consistently greater for C7(β)Δ*dtxR* and C7(β)*dtxR*-TnIN than for C7(β)*dtxR*-TnUP and C7(β), suggesting that growth under low-iron conditions does not result in complete inactivation of wild-type DtxR in the intracellular milieu. The repression ratio (the amount of toxin produced under low-iron conditions divided by the amount produced under high-iron conditions) ranged from 10 to 20 for C7(β), from 4 to 12 for C7(β)*dtxR*-TnUP, and from 0.5 to 2 for C7(β)Δ*dtxR* and C7(β)*dtxR*-TnIN. When pJKSdtxR was present, toxin production by all strains was usually repressed under high-iron conditions to levels comparable with those of C7(β), although some C7(β)Δ*dtxR* and C7(β)*dtxR*-TnIN transformants carrying pJKSdtxR continued to produce two to five times more toxin than C7(β) under high-iron conditions. Both C7(β) and *dtxR* mutant strains produced large and comparable amounts of siderophore under low-iron conditions (Fig. 2). Under high-iron conditions production of siderophore was strongly repressed in C7(β) and C7(β)*dtxR*-UP. Although C7(β)Δ*dtxR* and C7(β)*dtxR*-TnIN produced significantly less siderophore under high-iron conditions than under low-iron conditions, the amounts of siderophore that they produced under high-iron conditions were two to three times greater than those for C7(β) and C7(β)*dtxR*-UP (Fig. 2). The presence of pJKSdtxR in C7(β)Δ*dtxR* and C7(β)-*dtxR*-TnIN restored their ability to repress siderophore production under high-iron conditions,. These observations confirm previous findings with the transposon mutants (40), and they provide strong evidence that down-regulation of siderophore production in *C. diphtheriae* under high-iron growth conditions involves both DtxR-dependent and DtxR-independent mechanisms.

The final DtxR-dependent phenotypes that we examined were susceptibility to H_2O_2 in disk diffusion tests for growth inhibition performed on agar medium and in tests for killing performed in liquid medium. As previously reported (40), the phenotypes of C7(β)*dtxR*-TnUP and C7(β) were indistinguishable in these tests (data not shown). In contrast, the diameters of the zones of inhibition for C7(β)Δ*dtxR* and C7(β)*dtxR*-TnIN carrying the pJKS1 vector plasmid vector were approximately 20% greater than that for C7(β)/pJKS1. In addition the phenotype of C7(β)Δ*dtxR* was identical to that observed previously for C7(β)*dtxR*-TnIN in that both mutant strains were more susceptible than wild type to killing by H_2O_2 in liquid medium (data not shown and reference 40). When pJKSdtxR was present instead of pJKS1, the resistance of the mutant strains to killing by H_2O_2 was comparable to that of C7(β). Taken together, these findings demonstrated that the phenotype of C7(β)Δ*dtxR* is very similar to that of C7(β)*dtxR*-TnIN, and they indicate that possible polar effects of the transposon insertion in C7(β)*dtxR*-TnIN do not contribute significantly to the DtxR-dependent phenotypes tested in these experiments.

Transcripts containing *dtxR*. Previously, we reported preliminary evidence for a transcript that includes the 3′ end of

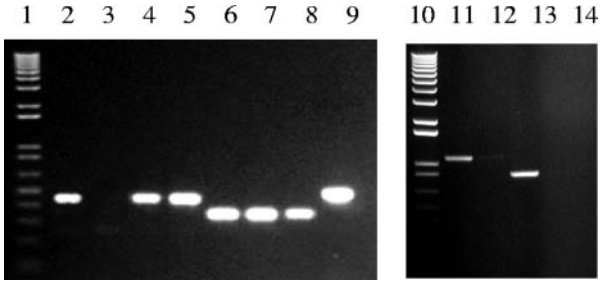

FIG. 3. Products of RT-PCR are shown. Lanes 1 and 10 contain a 1-kb Plus DNA ladder (Invitrogen), and lanes 2 to 9 and 11 to 14 contain the products of the RT-PCR performed with template RNA isolated from the following strains and the primers shown in Fig. 1: lane 2, C7(β), primers A and c; lane 3, C7(β)*dtxR*-TnUP, primers A and c; lane 4, C7(β)*dtxR*-TnIN primers A and c; lane 5, C7(β)Δ*dtxR*, primers A and c; lane 6, C7(β), primers E and b; lane 7, C7(β)*dtxR*-TnIN, primers E and b; lane 8, C7(β)*dtxR*-TnUP, primers E and b; lane 9, C7(β)Δ*dtxR*, primers D and b; lane 11, C7(β), primers B and b; lane 12, C7(β), primers B and b with no reverse transcriptase added; lane 13, C7(β)Δ*dtxR*, primers B and b; lane 14, C7(β)Δ*dtxR*, primers B and b with no reverse transcriptase added.

sigB and the 5′ end of *dtxR* (40). Here, we sought to confirm and extend this observation and also to investigate whether the *galE* gene, which starts only 22 bp downstream from the *dtxR* translational stop codon, can be cotranscribed with *dtxR*. Whole-cell RNAs from wild-type and mutant strains of *C. diphtheriae* were used as templates in reverse transcription reactions to generate cDNAs that initiated within *dtxR* and *galE*, respectively. The resulting cDNAs were used as templates to generate double-stranded PCR products that were analyzed by electrophoresis on agarose gels. With primers A and c, which are specific for the 3′ end of *sigB* and the 5′ end of *dtxR*, respectively (Fig. 1), a product of the expected size was detected with RNA from strains C7(β), C7(β)*dtxR*-TnIN, and C7(β)Δ*dtxR*, confirming the existence of a transcript extending from *sigB* into *dtxR*. No transcript was detected with primers A and c when RNA from C7(β)*dtxR*-TnUP was used as template because the transposon insertion in C7(β)*dtxR*-TnUP interrupts the chromosomal segment between primers A and c (Fig. 3). When primers specific for a *dtxR-galE* transcript were used [primers D and b for C7(β)Δ*dtxR* and primers E and b for all other strains (Fig. 1)], products of the expected sizes were detected in all strains, demonstrating the existence of a transcript that extends from *dtxR* into *galE* (Fig. 3). Finally we used primer b (which is identical to the 5′ end of *galE*) and primer B (which is identical to the 3′ end of *sigB*) to detect a transcript that includes all three genes shown in Fig. 1 (Fig. 3). Detection of these transcripts was not dependent on whether the cells from which RNA was isolated were starved for iron or not. In addition, control reactions without the reverse transcription step showed no products, indicating that the RNA samples were not contaminated with chromosomal DNA (data not shown and Fig. 3).

We attempted to detect *dtxR*-containing transcripts by using a *dtxR*-specific probe in Northern blots. As a control, we used a *tox*-specific probe and demonstrated a 1.8-kb *tox*-containing RNA transcript in whole-cell RNA isolated from C7(β) that was not present in RNA from C7(−), a nontoxinogenic strain that does not contain the *tox* gene encoded by phage β (13). As expected, the *tox* transcript was detected only when strains were grown under low-iron conditions (data not shown). When we used the *dtxR*-specific probe in the Northern blots, we sometimes detected a very faint band of approximately 1.7 kb, consistent with a transcript that included *dtxR* and *galE*, but we were unable to reproduce this result consistently. The occasional detection of this transcript did not depend on whether the RNA was isolated from iron-starved or iron-replete cells. These findings suggested that *dtxR*-specific transcripts in cells grown under low-iron or high-iron conditions were much less abundant than *tox*-specific transcripts in cells grown under low-iron conditions.

Transcriptional fusions. We began our study of the promoter(s) responsible for transcription of *dtxR*, *sigB*, and *galE* in *C. diphtheriae* by cloning several DNA fragments that included portions of the *sigB-dtxR* intergenic region from C7(β) and testing them for promoter activity in both *E. coli* and *C. diphtheriae* (Fig. 4). To assay the promoter activity of each DNA fragment, we used the transcriptional fusion vectors pQF50 (11) and pSPZ for assays in *E. coli* and *C. diphtheriae*, respectively. The pSPZ vector contains an origin of replication for *C. diphtheriae* and a promoterless *lacZ* reporter gene with upstream transcriptional terminators (see Materials and Methods). In both vectors, the DNA fragment of interest was cloned immediately upstream from *lacZ*, and promoter activity was determined by measuring β-galactosidase activity.

The largest clone, dtxRUP, included the final 465 bp of *sigB*, the 224-bp intergenic region between *dtxR* and *sigB*, and the first 25 bp of *dtxR* (Fig. 4A). The dtxRUP clone produced approximately 140 units of β-galactosidase activity in *E. coli*, and the activity of this promoter was not affected by the presence of either DtxR or iron (Fig. 4B and C). Under identical conditions, regulation of the *tox* promoter by DtxR and iron was confirmed with the positive control plasmid pQFtox (53). We constructed several subclones of the dtxRUP fragment to further localize the functional promoter (Fig. 4A). Subclone dtxRU1 has the same 3′ end as dtxRUP, but its 5′ end is the stop codon for *sigB* and it includes the entire *sigB-dtxR* intergenic region. Subclones dtxRU2 and dtxRU3 contain nonoverlapping upstream and downstream fragments of dtxRU1. Subclone dtxRU4 extends from the site of the transposon insertion in C7(β)*dtxR*-TnUP to the start codon of *dtxR*. Each of these subclones in pQF50 was tested for promoter activity in *E. coli* (Fig. 4B). The results localized the active *dtxR* promoter, P-dtxR, to a region within dtxRU3, demonstrated that dtxRU2 and dtxRU4 have no detectable promoter activity, and indicated that P-dtxR is more than 100 bp upstream from the translational start site of *dtxR*. We also tested pQF50 clones containing the DNA segments upstream of *sigB* (sigBUP) and *galE* (galEUP) (Fig. 4A) and demonstrated that they both lacked promoter activity in *E. coli* (Fig. 4C).

Finally, we tested clone dtxRU1 in pSPZ for promoter activity in wild-type *C. diphtheriae* C7(β) and in the C7(β)Δ*dtxR* mutant under high- and low-iron growth conditions, and we performed similar experiments in C7(β) with the sigBUP and galEUP clones (Fig. 4C). Clone dtxRU1 produced 20 to 30 Miller units of β-galactosidase activity, and its P-*dtxR* promoter was not regulated by DtxR or iron. In control experiments, however, the P-*tox* promoter did show the expected pattern of DtxR-dependent repression by iron. As in *E. coli*, the galEUP

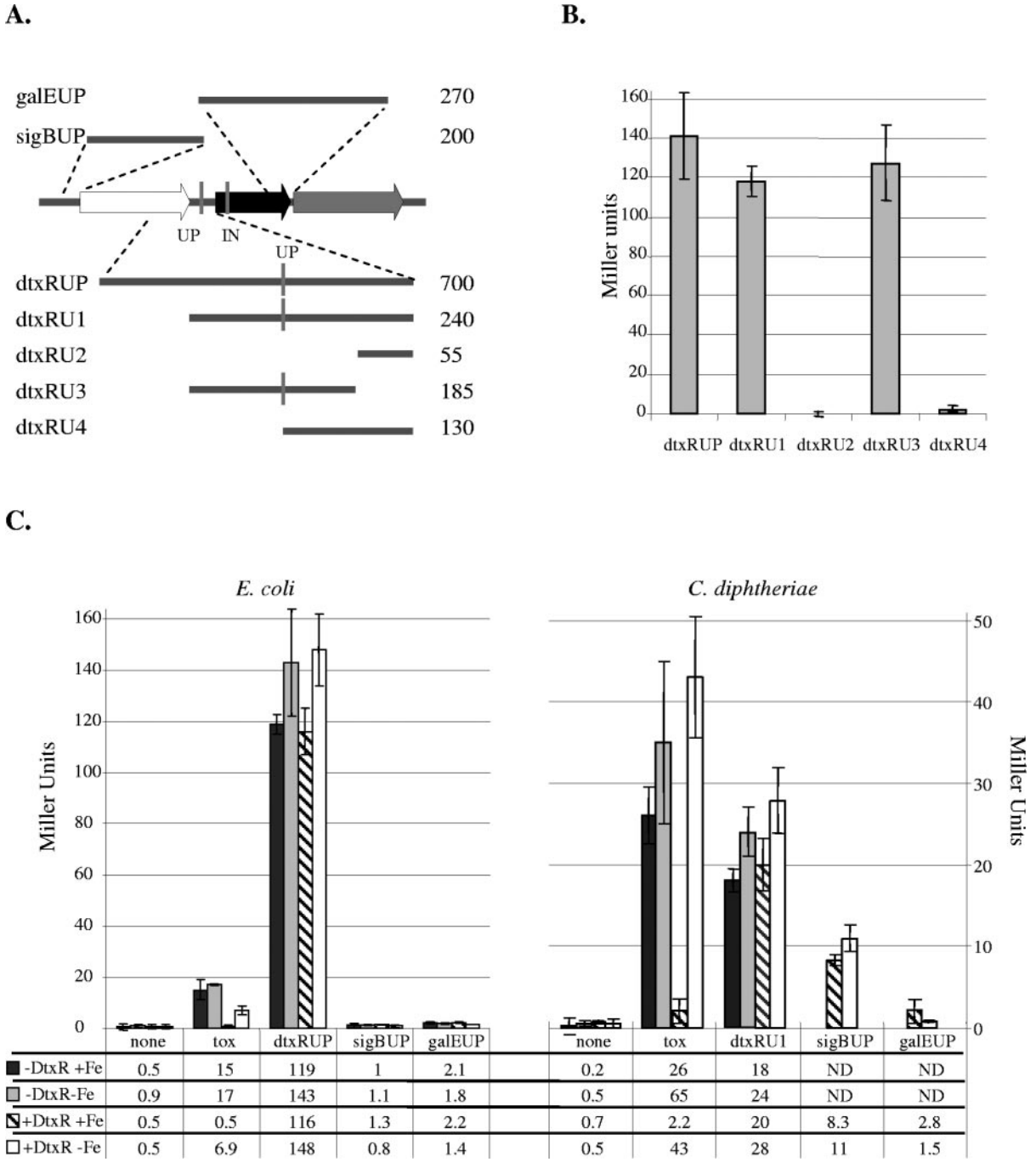

	E. coli					C. diphtheriae				
	none	tox	dtxRUP	sigBUP	galEUP	none	tox	dtxRU1	sigBUP	galEUP
-DtxR +Fe	0.5	15	119	1	2.1	0.2	26	18	ND	ND
-DtxR-Fe	0.9	17	143	1.1	1.8	0.5	65	24	ND	ND
+DtxR +Fe	0.5	0.5	116	1.3	2.2	0.7	2.2	20	8.3	2.8
+DtxR -Fe	0.5	6.9	148	0.8	1.4	0.5	43	28	11	1.5

FIG. 4. A. Maps of the regions from the *dtxR* locus assayed for promoter activity are shown. The genes and transposon insertions are indicated as in Fig. 1. The name of the DNA fragment is on the left, and the size in base pairs is indicated on the right. B. The promoter activity in *E. coli* (strain DH5α) of each *dtxR* promoter fragment listed at the bottom of the chart is indicated. C. The activity of each promoter fragment listed at the bottom of the chart is compared in *E. coli* (strain DH5α) and in *C. diphtheriae* [strains C7(β) and C7(β)Δ*dtxR*]. The DtxR expression phenotype of the host strain as well as the presence or absence of iron (Fe) in the assay medium is shown on the bottom left of each chart. All values are shown in Miller units, and ND indicates no data. Note the different scales on the vertical axes.

clone had no promoter activity. Although the sigBUP clone did not show any detectable promoter activity in *E. coli* (Fig. 4C), it did exhibit significant promoter activity in *C. diphtheriae* under both high-iron and low-iron growth conditions (Fig. 4C). We named the promoter contained on the sigBUP clone P-sigB.

Identification of the 5′ ends of transcripts encoding *dtxR* and *sigB*. First, we used RNase protection assays to identify the 5′ end of the transcript that initiates between *sigB* and *dtxR*. Three different ^{32}P-labeled single-stranded RNA probes were prepared that were complementary to different regions of the transcript within and upstream of *dtxR*. These probes were

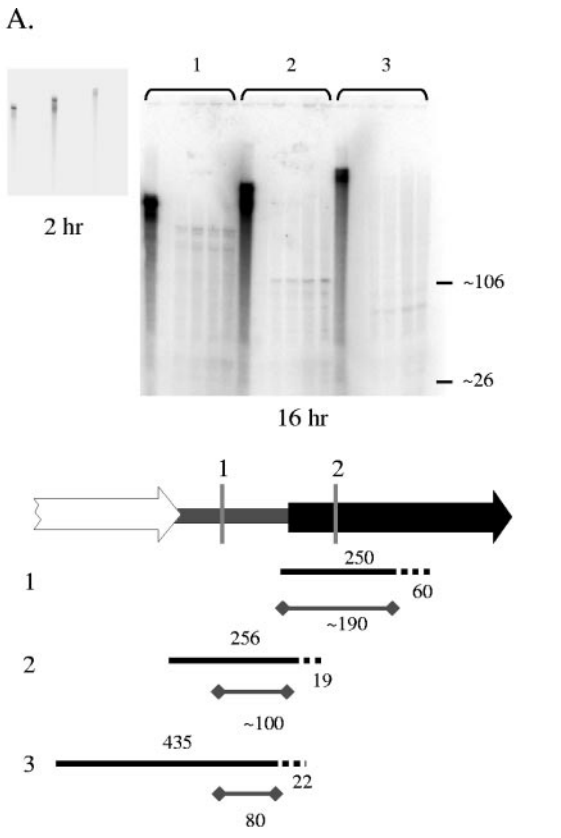

FIG. 5. A. RNase protection assays. The exposure time is indicated below each image. The positions of the xylene cyanol (~106 bases) and bromophenol blue (~26 bases) dyes on the gel are indicated on the right. For each probe (1 to 3) the first lane contains a reaction mixture in which nuclease was not included. The reaction mixtures were loaded in the following order: 2 μl probe plus yeast tRNA, 2 μl probe plus yeast tRNA, 2 μl probe plus 1 μg C7(β) RNA, 2 μl probe plus 2.5 μg C7(β) RNA, 10 μl probe plus 1 μg C7(β) RNA, 10 μl probe plus 2.5 μg C7(β) RNA. Under the gel images is a diagram indicating the input probe sizes and region protected from digestion. The input probe is shown as a black line (the dashed portion of the line is complementary to plasmid vector sequences rather than *C. diphtheriae* sequences). The region of each probe protected in the RNase assay is shown as a gray line with a diamond at each end. All sizes are shown in bases. B. Primer extension assays. The primer used to generate the sequencing ladder and the primer extension products is indicated. The lanes containing primer extension products are labeled + for template RNA isolated from high-iron cultures and − for template RNA isolated from low-iron cultures. The DNA sequence of the region between *sigB* and *dtxR* is shown below the images of the gels. The TAA stop codon of *sigB* and the ATG start codon of *dtxR* are capitalized and shown in boldface. The approximate region protected in the RNase assay is italicized. The site of the transposon insertion in C7(β)*dtxR*-TnUP is labeled UP. The base as the start site of *dtxR* transcription is labeled PE. The predicted −10 and −35 sequences of P-dtxR are capitalized and underlined.

then hybridized with RNA from C7(β) grown under high- or low-iron conditions, and the reaction products were digested with a mixture of RNase A and RNase T_1 and run on a 6% denaturing acrylamide gel. A scan of the gel obtained with a phosphoimager (Bio-Rad, Hercules, CA) is shown in Fig. 5A, along with a diagram that aids in the interpretation of the gel. The entire *C. diphtheriae*-specific region contained in probe 1 was protected from digestion, indicating that transcription initiated upstream of this probe's binding site. On the other hand, the ends of the *C. diphtheriae*-specific regions contained within probes 2 and 3 were not protected from digestion, indicating that probes 2 and 3 both overlapped the 5′ end of a *dtxR*-containing transcript. The sizes of the protected RNA fragments indicated that the 5′ end of that *dtxR*-containing transcript was located near the site of the transposon insertion in strain C7(β)*dtxR*-TnUP.

To localize the end of the transcript more precisely, we used RNA isolated from C7(β) as template in primer extension assays with primers that were labeled with ^{32}P at their 5′ ends. The resulting DNA products were run on 6% denaturing polyacrylamide gels next to sequencing ladders that were generated with the same primers (Fig. 5B). The results demonstrated that the 5′ end of the *dtxR*-containing transcript that initiates between *sigB* and *dtxR* is the C residue (note that the sequence in the figure is of the noncoding DNA strand) located 142 bp upstream of the *dtxR* ATG. The same 5′ end was identified using two different primers, and the detection of the primer extension product did not depend on whether the cells from which the RNA was isolated were starved for iron. In addition, we isolated RNA from *E. coli* cells containing the plasmid pQFdtxRUP (described above) and confirmed that the 5′ end of the *dtxR* transcript was the same in *E. coli* as in *C. diphtheriae* (data not shown). The DNA sequence of the *sigB-dtxR* intergenic region is also shown in Fig. 5B, and an *E. coli* σ^{70}-like −10 promoter-like sequence is properly positioned to direct initiation of transcription at the base identified by the primer extension experiments.

We also used primer extension assays to determine the 5′ end of the transcript that initiates upstream from *sigB*, within the sigBUP DNA fragment shown in Fig. 4A. Using RNA isolated from wild-type C7(β) grown under our standard high-iron and low-iron conditions (PGT medium with or without 10 μM of added $FeCl_3$), we were unable to detect any primer

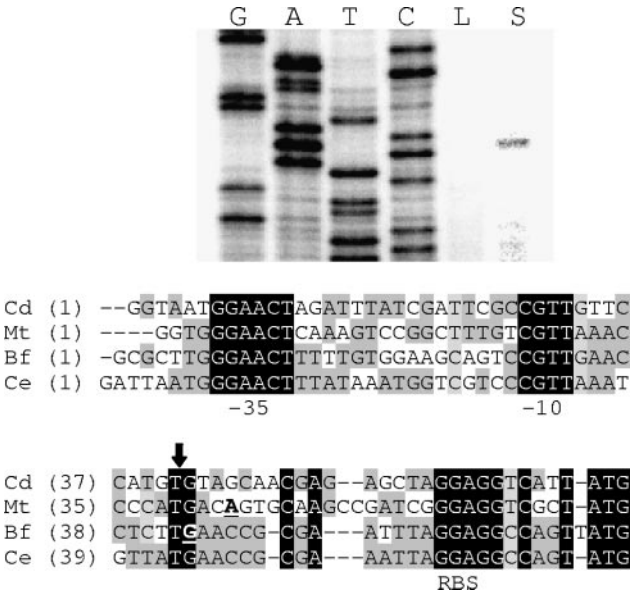

FIG. 6. The gel image includes the results of primer extension assays. The primer sigBPE3 was used to generate both the sequencing ladder (G, A, T, C) and the primer extension products. The lanes containing primer extension reaction mixtures are labeled L for template RNA isolated from low-iron cultures and S for template RNA isolated from low-iron cultures containing SDS. The DNA sequences of the regions upstream of *sigB* in *C. diphtheriae* (Cd), *M. tuberculosis* (Mt), *B. flavum* (Bf), and *Corynebacterium efficiens* (Ce) are shown below the image of the gel. The T residue corresponding to the start of the *sigB* transcript in *C. diphtheriae* is indicated by the vertical arrow. The underlined boldface bases in the Mt and Bf sequences indicate the previously reported transcript starts in those bacteria. The sequences corresponding to −10 and −35 sequences used by ECF sigma factors σ^E and σ^H are labeled. The proposed ribosome binding site is labeled RBS.

extension products. However, since transcription of *sigB* can be induced in *Mycobacterium* by stresses such as exposure to SDS (32), we also exposed C7(β) to SDS, isolated the RNA, and used that RNA in primer extension reactions with a *sigB*-specific primer. Figure 6 shows that the 5′ end of the *sigB*-containing transcript is the T residue located 26 bp upstream from the ATG start codon for *sigB* (as in Fig. 5, the sequencing ladder shown is for the noncoding strand). Figure 6 also compares the *sigB* promoter region of *C. diphtheriae* with homologous *sigB* promoters that are known to be regulated by extracytoplasmic function (ECF) sigma factors in several other actinomycete species. As will be discussed later, the hypothesis that *sigB* transcription is dependent on a corynebacterial ECF sigma factor is consistent with the observation that the sigBUP fragment has promoter activity only in *C. diphtheriae* and not in *E. coli*.

Quantitative analysis of transcripts containing *dtxR*, *sigB*, *galE*, and *tox*. We used real-time qRT-PCR to determine the relative amounts of *dtxR*-, *sigB*-, *galE*-, and *tox*-specific RNA transcripts and to investigate further the transcriptional regulation of these genes. We determined that transcripts specific for *sigA* (the primary σ^{70}-type sigma factor in *C. diphtheriae*) represented a constant fraction of total RNA during exponential growth, as reported previously for the closely related species *M. tuberculosis* (7) and *B. lactofermentum* (38), and we measured the other specific transcripts relative to the amount of *sigA*-specific transcripts. We examined *tox*-containing transcripts to confirm that the growth conditions used were sufficient to achieve transcriptional repression under high-iron conditions and derepression under low-iron conditions for this known DtxR-regulated gene. The positions of the probes and primers used for *dtxR* transcripts (probe DR, primers C and c), *sigB* transcripts (probe SB, primers B and d), *galE* transcripts (probe GE, primers G and a), and transcripts that span the *dtxR-galE* intergenic region (probe DG, primers F and b) are shown in Fig. 1, and the probes used for *sigA* and *tox* transcripts are described in Materials and Methods.

First, we determined the levels of *tox*, *dtxR*, and *sigB* transcripts at several points on the growth curves of *C. diphtheriae*, under low- and high-iron conditions. The quality of the RNA from cultures incubated longer than 15 h, as judged by smearing on ethidium bromide-stained agarose gels, was poor, so we did not include such samples in our analysis. The levels of each of these specific transcripts were usually significantly lower in samples from overnight cultures than in samples from log-phase and early-stationary-phase cultures (data not shown). The levels of transcripts for *sigB* and *dtxR* did not vary by more than 20% during the transition from log-phase growth to stationary phase and were similar under high-iron and low-iron conditions (Fig. 7A). In contrast, *tox*-containing transcripts did increase dramatically as cells growing under low-iron conditions exited from log phase, but there was no corresponding increase in *tox*-containing transcripts in cells growing under high-iron conditions. To investigate whether *tox* transcription was also regulated by growth phase, independently of its DtxR-dependent regulation by iron, we measured *tox* transcription under high- and low-iron conditions in strain C7(β)Δ*dtxR* at points on the growth curves corresponding with A to D in Fig. 7A (data not shown). During log-phase growth (point A), the levels of *tox* transcripts under both high- and low-iron growth conditions were approximately 25 units, comparable to the maximum levels observed during late log phase and early stationary phase under low-iron growth conditions in wild-type C7(β) (points B, C, and D in Fig. 7A). As the C7(β)Δ*dtxR* cells transitioned into stationary phase, the levels of *tox* transcripts increased progressively to approximately 65 units under both low- and high-iron conditions (data not shown). In the absence of DtxR-dependent regulation, therefore, the levels of *tox* transcripts did increase by two- to threefold, by mechanisms not yet determined, as the bacteria exited from log phase and entered stationary phase.

Next, we used qRT-PCR to compare the levels of *tox*-, *sigB*-, and *dtxR*-specific transcripts in *C. diphtheriae* strains C7(β), C7(β)*dtxR*-TnUP, C7(β)*dtxR*-TnIN, and C7(β)Δ*dtxR* under low- and high-iron conditions equivalent to point C on the growth curves in Fig. 7A (Table 2). In wild-type C7(β), expression of *tox* was strongly repressed by iron (repression ratios of 19 to 37). In contrast, transcript levels for *sigB* and *dtxR* were not significantly affected by iron (repression ratios of 0.8 to 1.5), and *dtxR*-specific transcripts were approximately threefold more abundant than *sigB*-specific transcripts. In addition, *tox*-specific transcripts were at least sixfold more abundant than *dtxR* transcripts under low-iron conditions, and they were threefold less abundant under high-iron conditions. Repression of *tox* transcription under high-iron conditions in C7(β)

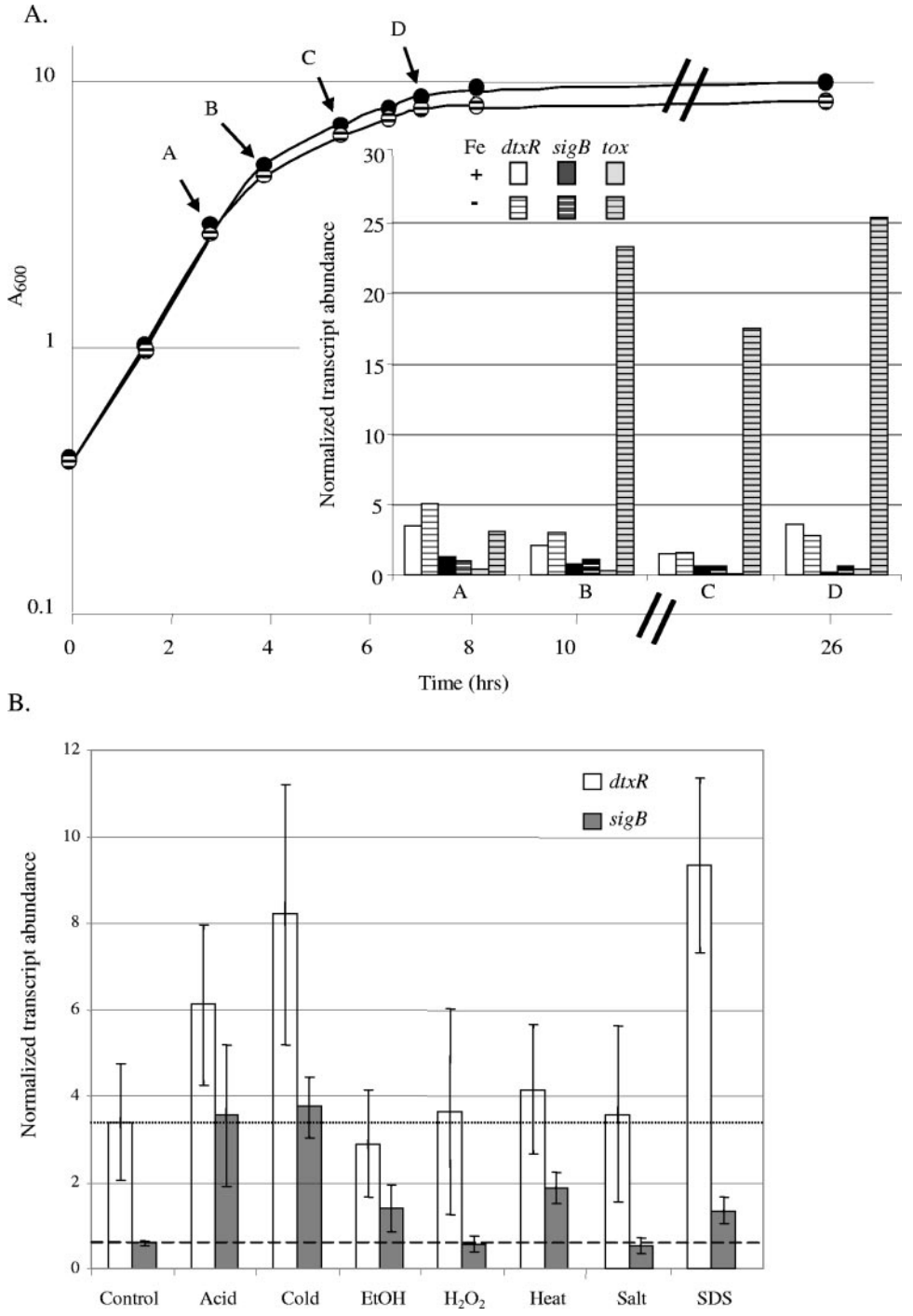

FIG. 7. (A) The growth curves of C7(β) in PGT (low-iron conditions, striped circles) and PGT plus 10 μM $FeCl_3$ (high-iron conditions, solid circles) media are shown. The abundance of transcripts measured by qRT-PCR with the probes indicated, normalized versus the abundance of *sigA* transcripts, is shown in the inset graph. The RNA used as a template in the qRT-PCR was isolated from samples of cultures harvested at the time points indicated in the growth curve (A, B, C, and D). Values obtained with RNA from high-iron cultures are shown by the solid bars, and values from low-iron RNA samples are shown by the striped bars. (B) Induction of specific transcripts (defined as normalized transcript abundance under stress conditions/normalized transcript abundance under control conditions) after exposure of C7(β) to indicated stress conditions is shown in the graph. The mean levels of *sigB* transcripts and *dtxR* transcripts under the low-iron control conditions are indicated by the dashed and dotted horizontal lines, respectively. The standard deviations between the values for three independent cultures are shown by the error bars. EtOH, ethanol.

dtxR-TnUP was less stringent and more variable (repression ratios of 4 to 30) than it was in wild-type C7(β), consistent with the phenotype described previously for C7(β)*dtxR*-TnUP and its lower intracellular level of DtxR. In C7(β) *dtxR*-TnIN and C7(β)Δ*dtxR*, transcription of *tox* was not iron regulated (repression ratios of 0.6 to 1.7), and the abundance of *tox* transcripts under both high- and low-iron conditions was two to three times greater than in C7(β) under low-iron conditions,

TABLE 2. Effects of iron on abundance of *tox*, *sigB*, and *dtxR* transcripts in wild-type and *dtxR* mutant strains of *C. diphtheriae*[a]

Strain	Value for transcript:								
	tox			*sigB*			*dtxR*		
	Low Fe	High Fe	Repression ratio	Low Fe	High Fe	Repression ratio	Low Fe	High Fe	Repression ratio
wt	13 ± 6	0.73 ± 0.7	19–37	0.67 ± 0.4	0.58 ± 0.3	0.8–1.5	2 ± 0.8	1.9 ± 0.5	0.9–1.5
UP	41 ± 51	7 ± 11	4–30	0.80 ± 0.5	0.83 ± 0.3	0.6–1.1	1.7 ± 0.3	1.6 ± 0.4	0.7–1.2
IN	34 ± 21	29 ± 18	0.7–1.7	1.1 ± 0.5	1.0 ± 0.5	0.7–1.7	1.8 ± 0.8	1.7 ± 0.7	0.7–1.5
ΔdtxR	40 ± 10	47 ± 21	0.6–1.2	1.1 ± 0.5	0.90 ± 0.5	0.5–1.7	3.2 ± 0.8	4.1 ± 1.1	0.5–1.2

[a] The strains from which RNA was isolated are listed in the stub: wt, C7(β); UP, C7(β)*dtxR*-TnUP; IN, *dtxR*-TnIN; ΔdtxR, C7(β)Δ*dtxR*. The level of each transcript was normalized to the level of the *sigA* transcript under high- or low-iron growth conditions (as described in Materials and Methods), and the data shown are the means and standard deviations for samples isolated from three independent cultures on the same day. The standard deviation of replicate reactions performed with the same input RNA was less than 2%, so the error introduced by the qRT-PCR assay itself was negligible. The range is shown for the repression ratios (low-iron/high-iron) among the three independent cultures.

consistent with incomplete derepression of *tox* transcription in C7(β) under low-iron conditions. The abundance of *sigB* transcripts in all three mutants was comparable to that in wild-type C7(β). The average abundance of *dtxR* transcripts was comparable in C7(β) and C7(β)*dtxR*-TnIN, trended toward slightly lower values in C7(β)*dtxR*-TnUP, and was approximately twofold greater in C7(β)Δ*dtxR*. Although the lower average levels of *dtxR* transcription in C7(β)*dtxR*-TnUP were consistent with its observed phenotype of lower DtxR production (40), the differences from wild type were not statistically significant. The *dtxR* transcripts in C7(β)Δ*dtxR* differed in structure from those in the other strains because of the internal deletion in *dtxR* located downstream from the location of the DR probe (Fig. 1), and this difference may have affected stability or production of *dtxR* transcripts in C7(β)Δ*dtxR*.

We also used qRT-PCR to investigate further whether *galE* is cotranscribed with *dtxR* or is transcribed from an independent promoter that was not detected in our previous experiments (Fig. 4). We used probe DG with primers F and b to detect transcripts that extend from the 3′ end of *dtxR* into the 5′ end of *galE* and probe GE with primers G and a to detect transcripts of an internal region of the coding sequence for *galE* (Fig. 1). If *galE* can be transcribed both from a promoter in the *dtxR-galE* intergenic region and also by extension of *dtxR*-specific transcripts that initiate further upstream, then the transcripts detected by the GE probe should be more abundant than the transcripts detected by the DG probe. The results of our qRT-PCR assays on RNA from three independent cultures grown under both high- and low-iron conditions revealed that transcripts including the 3′ end of *dtxR* and the 5′ end of *galE* were slightly more abundant (1.8 ± 0.6 times), rather than less abundant, than those corresponding to the internal sequence in *galE*. These results are most consistent with the hypothesis that *galE* is cotranscribed with *dtxR* but not also transcribed from a *galE*-only promoter.

Finally, we tested several different stress conditions, some of which are known to affect transcription of *sigB* in other actinomycetes, for their effect on transcription of *dtxR* and *sigB* in *C. diphtheriae*. We exposed exponentially growing *C. diphtheriae* to acid, cold, ethanol, H_2O_2, heat, salt, or SDS for 35 min and then isolated whole-cell RNA. We assayed each sample for *sigB*- and *dtxR*-specific transcripts, once again normalizing them to the amounts of *sigA*-specific transcripts (Fig. 7B). The mean abundance for transcripts of each gene during growth under low-iron control conditions is shown by the first set of data bars and also by the dashed horizontal line for *sigB* transcripts and the dotted horizontal line for *dtxR* transcripts. Under these control conditions, *dtxR*-specific transcripts were four- to fivefold more abundant than *sigB*-specific transcripts. Significant increases in mean levels of *sigB* transcripts were observed after exposure to acid (~5-fold), cold (~6-fold), ethanol (~2-fold), heat (~3-fold), or SDS (~2-fold), but no significant increases were seen after exposure to H_2O_2 or salt. In contrast, significant increases in mean levels of *dtxR* transcripts were observed only after exposure to acid (~2-fold), cold (2- to 3-fold), or SDS (~3-fold). For acid and cold stress conditions, the increase in *dtxR* transcripts could potentially be due to extension of *sigB*-containing transcripts. In contrast, under SDS stress conditions, the increase in *sigB*-containing transcripts was not large enough for extension of *sigB*-containing transcripts to serve as a possible explanation for the observed increase in *dtxR*-containing transcripts.

DISCUSSION

Until recently, the molecular and genetic tools required to dissect the nuances of transcriptional regulation in the *Actinomycetales* order of bacteria were not readily available. Among the actinomycetes, several families in the *Corynebacteriaceae* suborder (i.e., *Mycobacteriaceae*, *Nocardiaceae*, *Rhodococcus*, and *Corynebacteriaceae*) contain species classified as human pathogens, so understanding transcriptional regulation in this order of bacteria is of interest not only to microbial geneticists but also to investigators committed to understanding and developing new antimicrobials directed against bacterial pathogens.

While characterizing transcription in and around the chromosomal locus for *dtxR*, we uncovered several new and fascinating features of transcriptional regulation in *Corynebacterium diphtheriae*. There are 224 bp between *dtxR* and the gene encoded immediately upstream, *sigB*. Although we found no evidence of promoter activity within the 150-bp segment immediately upstream of *dtxR*, we demonstrated an active promoter further upstream in this intergenic region that directs transcription to initiate at a C located 142 bases upstream of the start codon for *dtxR*. Transcription initiation controlled by this promoter, P-dtxR, both in *E. coli* and in *C. diphtheriae* is not affected by the presence of DtxR or the concentration of iron in the growth medium. In contrast, the promoters from *C. diphtheriae* that have been characterized previously were cho-

sen for study because they exhibit DtxR-dependent negative regulation by iron both in *E. coli* and in *C. diphtheriae* (3, 28, 43, 53, 54), and in the case of the *hmuO* promoter repression of transcription requires iron-activated DtxR while full activation requires the presence of heme (50). Furthermore, the position of P-dtxR, over 150 bases upstream of *dtxR*, results in a much larger untranslated region (142 bases) than any of the other transcripts from *C. diphtheriae* for which start sites have been mapped. For example, the transcriptional start sites for P-tox, IRP1, and the *hmuO* promoter are 40, 35, and 47 bases upstream from their respective translational start codons (29, 50, 56). The significance of the longer untranslated region in the mRNA transcript that begins at P-dtxR is unknown. We also scanned the region between *sigB* and *dtxR* for sites with homology to the consensus DtxR binding site, and one site with greater than 60% identity was identified. This site matches the consensus DtxR binding sequence at 12 of the 19 nucleotide positions and is centered 63 nucleotides upstream of the transcriptional start and 206 nucleotides upstream of the translational start of *dtxR*. The low homology of this site with the consensus DtxR binding site as well as its location far upstream from P-dtxR make it unlikely to be involved in regulation of transcription of P-dtxR, and we found no evidence of DtxR-dependent transcription in this region.

When the DNA sequence in the P-dtxR region was scanned for promoter-like −10 and −35 elements, candidate sequences were easily identified. A −10 sequence identical to the consensus −10 (TATAAT) for the primary σ^{70}-type promoters in *E. coli* (σ^{70}) and *B. subtilis* (σ^{A}) is shown in Fig. 5. The TT aAaA −35 sequence matches the TTGACA −35 consensus sequence for primary σ^{70}-type promoters at four of six positions. The spacing between the −10 and −35 sequences of P-dtxR is 20 bases, whereas the spacing for the vast majority of σ^{70}-type promoters is 16 to 18 bases. The sequences in the P-dtxR region were also compared to promoter sequences from other actinomycete species. In *Corynebacterium glutamicum*, an extended −10 consensus sequence, tgngnTA(c/t)a aTgg (the bases shown as lowercase occur in at least 40% of the promoters and bases shown as uppercase occur in more than 70% of promoters), was identified by analyzing 53 different promoters (42). The P-dtxR −10 promoter sequence gGcGtTATAATta (Fig. 5) matches this consensus sequence at 8 of the 11 positions (ignoring the positions at which any base *n* is acceptable), including all three bases conserved in greater than 70% of the promoters. The −35 region of *C. glutamicum* promoters is much less conserved than the −35 regions of *E. coli* and *B. subtilis* promoters, and the extended −10 region appears to be more important than the −35 sequence for promoter recognition in that species. In *M. tuberculosis*, the consensus sequence for promoters recognized by the primary sigma factor σ^{A} is TTGAC(A/T)-N17-TATA(A/C)T (62). This consensus is nearly identical to those for *E. coli* σ^{70} and *B. subtilis* σ^{A}. Although the sequences in and around P-dtxR appear to be most similar to those observed in *C. glutamicum* promoters, our experiments demonstrated that P-dtxR can function in *E. coli* to direct transcription initiating at the same base as in *C. diphtheriae*, notwithstanding the poor match and spacing of its −35 region with the consensus −35 region for *E. coli*. Whether the atypical spacing between the −10 and −35 regions of P-dtxR is a factor in determining the abundance of the *dtxR*-specific transcripts that initiate from P-dtxR remains to be determined.

Transcription of *dtxR* was unaffected by most growth conditions. The exceptions were exposure to acid, cold, or SDS, each of which caused transcription of *dtxR* to increase by two- to threefold (Fig. 7B). The increase in *dtxR* transcription following exposure to acid or cold could be due to the five- to sixfold increase in transcription of *sigB* under those conditions if most or all of the *sigB*-containing transcripts extended through *dtxR*. On the other hand, the increase in *sigB* transcription after exposure to SDS was too small to serve as the primary mechanism for the concomitant increase in *dtxR*-containing transcripts. To investigate whether transcription of *dtxR* in the presence of SDS was the result of the activity of P-dtxR or of a separate SDS-responsive promoter in the *sigB-dtxR* intergenic region, we repeated the primer extension analysis with RNA isolated under SDS stress conditions. The transcription start site identified with the RNA from SDS-stressed cultures was identical to that found under all other conditions tested (data not shown). These results suggest that the *dtxR* transcripts observed in the presence of SDS arise primarily as the result of transcription initiating at P-dtxR.

Although multiple mechanisms may mediate the increase in transcription of *dtxR* in response to the various stress conditions that we studied, it is possible that transcription of *dtxR* and the *galE* gene located immediately downstream is affected by changes in the cell surface. The role of the *galE* gene product in *C. diphtheriae* physiology has not been determined, but it demonstrates homology with UDP-galactose 4-epimerases of other bacteria. GalE enzymes catalyze the interconversion of UDP-galactose and UDP-glucose. In other bacterial species, UDP-galactose and UDP-glucose are substrates for the production of exopolysaccharides on the surface of the cell (26, 63). Since it is possible that the *galE* gene product is required to synthesize a cell surface polysaccharide, it is reasonable to speculate that transcription of *galE* as part of a polycistronic message controlled by P-dtxR or P-sigB or both might be responsive to changes in the cell surface.

In addition to the *dtxR*-containing transcript that initiates from P-dtxR, our analysis of mRNAs in this region demonstrated that a second transcript spans the 3′ end of *sigB* and the 5′ end of *dtxR* and that this transcript must initiate at least 800 bases upstream of *dtxR*. Since it seemed likely that this second *dtxR*-containing transcript included *sigB*, we tested the region upstream of *sigB* for promoter activity. We determined that the promoter located upstream of *sigB* was active only in *C. diphtheriae* and not in *E. coli*. In addition the number of transcripts containing *sigB* was induced by several environmental conditions, including exposure to acid, cold, heat, ethanol, or SDS. Exposure to salt or hydrogen peroxide had no effect on transcription of *sigB* (Fig. 7B). These findings suggested that the promoter upstream of *sigB* may be recognized by an ECF sigma factor, similar to ones that have been shown to coordinate gene transcription in response to various stress conditions in many other bacterial species (20).

In the *C. diphtheriae* genome there are nine annotated sigma factor genes, all of which are in the σ^{70} family (4). Using the numbering scheme from the published genome, the primary sigma factor σ^{A} is encoded by DIP1406 and σ^{B} is encoded by DIP1413. This gene arrangement with *sigA* and *sigB* encoded

near one another is also seen in other actinomycetes such as *M. tuberculosis*. In *M. tuberculosis*, *sigB* transcription is controlled by two different ECF sigma factors, σ^E and σ^H (31, 32). These two ECF sigma factors of *M. tuberculosis* use the same promoter sequences upstream of *sigB*, but they differ with respect to the conditions under which they are active. Specifically, the consensus sequence for binding of RNA polymerase holoenzyme including σ^E is a −35 sequence of GG(A/G)(A/C)C and a −10 sequence of (G/C)GTTG (32), and the sequence recognized by RNA polymerase holoenzyme including σ^H is a −35 sequence equal to (G/C)GGAAC and a −10 sequence of (G/C)GTT(G/C) (31). σ^E is required for the increase in *sigB* expression following exposure to SDS (32), while σ^H is required for the increase in *sigB* expression following exposure to heat (31). *C. diphtheriae* encodes homologues of σ^E (DIP0994) and σ^H (DIP0709), and as shown in Fig. 6, the P-sigB promoter contains sequences that are homologous to the consensus sequences determined for these two ECF sigma factors.

Transcription dependent on σ^H has been demonstrated in *C. glutamicum*, a species used to produce amino acids on an industrial scale. In *C. glutamicum*, transcription of four genes whose products have a role in the function of the ATP-dependent protease Clp was induced by heat shock. The promoters for these genes all contain the consensus −10 and −35 sequences (shown in Fig. 6) for σ^E and σ^H. Finally, inactivation of *sigH* prevented induction of transcription of all four genes by heat shock (10). These findings provide clear evidence for ECF sigma factor function in *Corynebacterium* and support the theory that *sigB* in *C. diphtheriae* is likely transcribed by an RNA polymerase holoenzyme that contains either σ^E or σ^H.

Transcription of *sigB* has also been investigated in the actinomycete genus *Brevibacterium*, which is closely related to *Corynebacterium*. In both *B. flavum* and *B. lactofermentum*, the start site for *sigB* transcription has been mapped to a G located 24 bp upstream of the ATG, and these start sites are nearly identical to the site we identified in *C. diphtheriae* (Fig. 6) (17, 38). The DNA sequences upstream of *sigB* in the closely related species *B. flavum*, *B. lactofermentum*, and *C. glutamicum* are identical, so only the *B. flavum* sequence was included in Fig. 6. In *B. flavum*, transcription of *sigB* was shown to be increased after acid stress, cold shock, and exposure to ethanol, all of which also increased transcription of *sigB* in *C. diphtheriae*. In addition, inactivation of *sigB* in *B. flavum* caused increased sensitivity to acid, salt, ethanol, heat, and cold stress, indicating that σ^B likely has a role in the environmental stress response (18). This observation correlates with our findings that the transcription of *sigB* is increased in response to these environmental stress conditions (Fig. 7B).

All of our data indicate that *dtxR* and *galE* are encoded on the same transcript in *C. diphtheriae*, and we could find no evidence of a *galE*-only promoter (i.e., a promoter in the intergenic region between *dtxR* and *galE*). These findings are in agreement with observations in *B. lactofermentum*, where *dmdR* (the *dtxR* homologue) and *galE* are cotranscribed (36). The gene arrangement at the *dtxR* locus is conserved among the members of the genus *Corynebacterium* for which genome sequencing has been completed (24, 35). Also consistent with our observation that there is a transcript that includes the 3′ end of *sigB* and the 5′ end of *dtxR* in *C. diphtheriae*, a transcript that spans the intergenic region between *sigB* and *dmdR* was observed in *B. lactofermentum* (38). Additionally we provide evidence that in *C. diphtheriae* there is cotranscription of *sigB*, *dtxR*, and *galE*. There is a difference between the gene arrangement at the *ideR* locus (equivalent to the *dtxR* locus) found in the genus *Mycobacterium* and that present in *Corynebacterium*. In both *M. tuberculosis* and *Mycobacterium bovis*, the gene order of *sigB* and *ideR* is identical to that seen in *Corynebacterium* but the gene immediately downstream of *ideR* is not *galE* (5, 14). Instead, a gene of unknown function is encoded downstream of *ideR* on the opposite DNA strand. Therefore, *ideR* in *Mycobacterium* does not appear to be cotranscribed with any other downstream gene.

In summary, we have demonstrated that transcriptional regulation of the genes in the *C. diphtheriae dtxR* locus is a multifaceted process that is affected by several environmental factors. We have mapped and characterized two new promoters from *C. diphtheriae*, P-dtxR and P-sigB. Of these, P-sigB is the first promoter from *C. diphtheriae* likely to be recognized by an RNA polymerase holoenzyme that contains an ECF sigma factor. ECF sigma factors direct transcription in response to extracellular signals, and *sigB* transcript levels were shown to increase in response to acid stress, ethanol exposure, heat shock, cold shock, or exposure to SDS. Transcription initiation at P-dtxR results in a *dtxR*-containing transcript that includes 142 bases of untranslated mRNA, the role of which remains to be determined. By analyzing the transcripts that include *dtxR*, we showed that *sigB*, *dtxR*, and *galE* are cotranscribed. Finally, although transcription of *dtxR* was not dramatically affected by several extracellular signals, we did observe an increase in *dtxR*-containing transcripts in response to exposure to acid, cold, or SDS, which may indicate that transcription of these genes is responsive to changes in the cell envelope or surface stress.

ACKNOWLEDGMENTS

This work was supported in part by grant number AI14107 from the National Institute of Allergy and Infectious Diseases (to R.K.H.) and by a postdoctoral fellowship awarded to D.M.O. under training grant AI07587 from the National Institute of Allergy and Infectious Diseases.

We thank Farrah M. Clemens for designing the fluorescent probe and primers used to detect *sigA*-containing transcripts and Mark Oram for critical reading of and advice on the manuscript.

REFERENCES

1. **Barksdale, L. W., and A. M. J. Pappenheimer.** 1954. Phage-host relationships in nontoxigenic and toxigenic diphtheria bacilli. J. Bacteriol. **67:**220–232.
2. **Boland, C. A., and W. G. Meijer.** 2000. The iron dependent regulatory protein IdeR (DtxR) of *Rhodococcus equi*. FEMS Microbiol. Lett. **191:**1–5.
3. **Boyd, J., M. N. Oza, and J. R. Murphy.** 1990. Molecular cloning and DNA sequence analysis of a diphtheria tox iron-dependent regulatory element (*dtxR*) from *Corynebacterium diphtheriae*. Proc. Natl. Acad. Sci. USA **87:** 5968–5972.
4. **Cerdeno-Tarraga, A. M., A. Efstratiou, L. G. Dover, M. T. Holden, M. Pallen, S. D. Bentley, G. S. Besra, C. Churcher, K. D. James, A. De Zoysa, T. Chillingworth, A. Cronin, L. Dowd, T. Feltwell, N. Hamlin, S. Holroyd, K. Jagels, S. Moule, M. A. Quail, E. Rabbinowitsch, K. M. Rutherford, N. R. Thomson, L. Unwin, S. Whitehead, B. G. Barrell, and J. Parkhill.** 2003. The complete genome sequence and analysis of *Corynebacterium diphtheriae* NCTC13129. Nucleic Acids Res. **31:**6516–6523.
5. **Cole, S. T., R. Brosch, J. Parkhill, T. Garnier, C. Churcher, D. Harris, S. V. Gordon, K. Eiglmeier, S. Gas, C. E. Barry III, F. Tekaia, K. Badcock, D. Basham, D. Brown, T. Chillingworth, R. Connor, R. Davies, K. Devlin, T. Feltwell, S. Gentles, N. Hamlin, S. Holroyd, T. Hornsby, K. Jagels, B. G. Barrell, et al.** 1998. Deciphering the biology of *Mycobacterium tuberculosis* from the complete genome sequence. Nature **393:**537–544.

6. **Doukhan, L., M. Predich, G. Nair, O. Dussurget, I. Mandic-Mulec, S. T. Cole, D. R. Smith, and I. Smith.** 1995. Genomic organization of the mycobacterial sigma gene cluster. Gene **165:**67–70.
7. **Dubnau, E., P. Fontan, R. Manganelli, S. Soares-Appel, and I. Smith.** 2002. *Mycobacterium tuberculosis* genes induced during infection of human macrophages. Infect. Immun. **70:**2787–2795.
8. **Dussurget, O., M. Rodriguez, and I. Smith.** 1996. An *ideR* mutant of *Mycobacterium smegmatis* has derepressed siderophore production and an altered oxidative-stress response. Mol. Microbiol. **22:**535–544.
9. **Dussurget, O., J. Timm, M. Gomez, B. Gold, S. Yu, S. Z. Sabol, R. K. Holmes, W. R. Jacobs, and I. Smith.** 1999. Transcriptional control of the iron-responsive *fxbA* gene by the mycobacterial regulator IdeR. J. Bacteriol. **181:**3402–3408.
10. **Engels, S., J. E. Schweitzer, C. Ludwig, M. Bott, and S. Schaffer.** 2004. *clpC* and *clpP1P2* gene expression in *Corynebacterium glutamicum* is controlled by a regulatory network involving the transcriptional regulators ClgR and HspR as well as the ECF sigma factor σ^H. Mol. Microbiol. **52:**285–302.
11. **Farinha, M. A., and A. M. Kropinski.** 1990. Construction of broad-host-range plasmid vectors for easy visible selection and analysis of promoters. J. Bacteriol. **172:**3496–3499.
12. **Feese, M. D., E. Pohl, R. K. Holmes, and W. G. J. Hol.** 2001. Iron-dependent regulators, p. 850–863. *In* A. Messerschmidt, R. Huber, R. Poulos, and K. Wieghardt (ed.), Handbook of metalloproteins. John Wiley & Sons, Ltd., Chichester, United Kingdom.
13. **Freeman, V. J.** 1951. Studies on the virulence of bacteriophage-infected strains of *Corynebacterium diphtheriae*. J. Bacteriol. **61:**675–688.
14. **Garnier, T., K. Eiglmeier, J. C. Camus, N. Medina, H. Mansoor, M. Pryor, S. Duthoy, S. Grondin, C. Lacroix, C. Monsempe, S. Simon, B. Harris, R. Atkin, J. Doggett, R. Mayes, L. Keating, P. R. Wheeler, J. Parkhill, B. G. Barrell, S. T. Cole, S. V. Gordon, and R. G. Hewinson.** 2003. The complete genome sequence of *Mycobacterium bovis*. Proc. Natl. Acad. Sci. USA **100:**7877–7882.
15. **Gold, B., G. M. Rodriguez, S. A. Marras, M. Pentecost, and I. Smith.** 2001. The *Mycobacterium tuberculosis* IdeR is a dual functional regulator that controls transcription of genes involved in iron acquisition, iron storage and survival in macrophages. Mol. Microbiol. **42:**851–865.
16. **Gunter-Seeboth, K., and T. Schupp.** 1995. Cloning and sequence analysis of the *Corynebacterium diphtheriae dtxR* homologue from *Streptomyces lividans* and *S. pilosus* encoding a putative iron repressor protein. Gene **166:**117–119.
17. **Halgasova, N., G. Bukovska, J. Timko, and J. Kormanec.** 2001. Cloning and transcriptional characterization of two sigma factor genes, *sigA* and *sigB*, from *Brevibacterium flavum*. Curr. Microbiol. **43:**249–254.
18. **Halgasova, N., G. Bukovska, J. Ugorcakova, J. Timko, and J. Kormanec.** 2002. The *Brevibacterium flavum* sigma factor SigB has a role in the environmental stress response. FEMS Microbiol. Lett. **216:**77–84.

18a. **Hantke, K.** 2001. Iron and metal regulation in bacteria. Curr. Opin. Microbiol. **4:**172–177.

19. **Hardham, J. M., L. V. Stamm, S. F. Porcella, J. G. Frye, N. Y. Barnes, J. K. Howell, S. L. Mueller, J. D. Radolf, G. M. Weinstock, and S. J. Norris.** 1997. Identification and transcriptional analysis of a *Treponema pallidum* operon encoding a putative ABC transport system, an iron-activated repressor protein homolog, and a glycolytic pathway enzyme homolog. Gene **197:**47–64.
20. **Helmann, J. D.** 2002. The extracytoplasmic function (ECF) sigma factors. Adv. Microb. Physiol. **46:**47–110.
21. **Hill, P. J., A. Cockayne, P. Landers, J. A. Morrissey, C. M. Sims, and P. Williams.** 1998. SirR, a novel iron-dependent repressor in *Staphylococcus epidermidis*. Infect. Immun. **66:**4123–4129.
22. **Holmes, R. K.** 2000. Biology and molecular epidemiology of diphtheria toxin and the *tox* gene. J. Infect. Dis. **181:**S156–S167.
23. **Hu, Y., and A. R. M. Coates.** 1999. Transcription of two sigma 70 homologue genes, *sigA* and *sigB*, in stationary-phase *Mycobacterium tuberculosis*. J. Bacteriol. **181:**469–476.
24. **Kalinowski, J., B. Bathe, D. Bartels, N. Bischoff, M. Bott, A. Burkovski, N. Dusch, L. Eggeling, B. J. Eikmanns, L. Gaigalat, A. Goesmann, M. Hartmann, K. Huthmacher, R. Kramer, B. Linke, A. C. McHardy, F. Meyer, B. Mockel, W. Pfefferle, A. Puhler, D. A. Rey, C. Ruckert, O. Rupp, H. Sahm, V. F. Wendisch, I. Wiegrabe, and A. Tauch.** 2003. The complete *Corynebacterium glutamicum* ATCC 13032 genome sequence and its impact on the production of L-aspartate-derived amino acids and vitamins. J. Biotechnol. **104:**5–25.
25. **Kitten, T., C. L. Munro, S. M. Michalek, and F. L. Macrina.** 2000. Genetic characterization of a *Streptococcus mutans* LraI family operon and role in virulence. Infect. Immun. **68:**4441–4451.
26. **Kleerebezem, M., R. van Kranenburg, R. Tuinier, I. C. Boels, P. Zoon, E. Looijesteijn, J. Hugenholtz, and W. M. de Vos.** 1999. Exopolysaccharides produced by *Lactococcus lactis*: from genetic engineering to improved rheological properties? Antonie Leeuwenhoek **76:**357–365.
27. **Kunkle, C. A., and M. P. Schmitt.** 2003. Analysis of the *Corynebacterium diphtheriae* DtxR regulon: identification of a putative siderophore synthesis and transport system that is similar to the *Yersinia* high-pathogenicity island-encoded yersiniabactin synthesis and uptake system. J. Bacteriol. **185:**6826–6840.
28. **Lee, J. H., T. Wang, K. Ault, J. Liu, M. P. Schmitt, and R. K. Holmes.** 1997. Identification and characterization of three new promoter/operators from *Corynebacterium diphtheriae* that are regulated by the diphtheria toxin repressor (DtxR) and iron. Infect. Immun. **65:**4273–4280.
29. **Leong, D., and J. R. Murphy.** 1985. Characterization of the diphtheria *tox* transcript in *Corynebacterium diphtheriae* and *Escherichia coli*. J. Bacteriol. **163:**1114–1119.
30. **Love, J. F., J. C. vanderSpek, V. Marin, L. Guerrero, T. M. Logan, and J. R. Murphy.** 2004. Genetic and biophysical studies of diphtheria toxin repressor (DtxR) and the hyperactive mutant DtxR(E175K) support a multistep model of activation. Proc. Natl. Acad. Sci. USA **101:**2506–2511.
31. **Manganelli, R., M. I. Voskuil, G. K. Schoolnik, E. Dubnau, M. Gomez, and I. Smith.** 2002. Role of the extracytoplasmic-function σ factor σ^H in *Mycobacterium tuberculosis* global gene expression. Mol. Microbiol. **45:**365–374.
32. **Manganelli, R., M. I. Voskuil, G. K. Schoolnik, and I. Smith.** 2001. The *Mycobacterium tuberculosis* ECF sigma factor σ^E: role in global gene expression and survival in macrophages. Mol. Microbiol. **41:**423–437.
33. **Miller, J. H.** 1972. Experiments in molecular genetics. Cold Spring Harbor Laboratory, Cold Spring Harbor, N.Y.
34. **Mothershed, E. A., P. K. Cassiday, K. Pierson, L. W. Mayer, and T. Popovic.** 2002. Development of a real-time fluorescence PCR assay for rapid detection of the diphtheria toxin gene. J. Clin. Microbiol. **40:**4713–4719.
35. **Nishio, Y., Y. Nakamura, Y. Kawarabayasi, Y. Usuda, E. Kimura, S. Sugimoto, K. Matsui, A. Yamagishi, H. Kikuchi, K. Ikeo, and T. Gojobori.** 2003. Comparative complete genome sequence analysis of the amino acid replacements responsible for the thermostability of *Corynebacterium efficiens*. Genome Res. **13:**1572–1579.
36. **Oguiza, J. A., A. T. Marcos, M. Malumbres, and J. F. Martin.** 1996. The *galE* gene encoding the UDP-galactose 4-epimerase of *Brevibacterium lactofermentum* is coupled transcriptionally to the *dmdR* gene. Gene **177:**103–107.
37. **Oguiza, J. A., A. T. Marcos, M. Malumbres, and J. F. Martin.** 1996. Multiple sigma factor genes in *Brevibacterium lactofermentum*: characterization of *sigA* and *sigB*. J. Bacteriol. **178:**550–553.
38. **Oguiza, J. A., A. T. Marcos, and J. F. Martin.** 1997. Transcriptional analysis of the *sigA* and *sigB* genes of *Brevibacterium lactofermentum*. FEMS Microbiol. Lett. **153:**111–117.
39. **Oram, D. M., A. Avdalovic, and R. K. Holmes.** 2004. Analysis of genes that encode DtxR-like transcriptional regulators in pathogenic and saprophytic corynebacterial species. Infect. Immun. **72:**1885–1895.
40. **Oram, D. M., A. Avdalovic, and R. K. Holmes.** 2002. Construction and characterization of transposon insertion mutations in *Corynebacterium diphtheriae* that affect expression of the diphtheria toxin repressor (DtxR). J. Bacteriol. **184:**5723–5732.
41. **Oram, D. M., L. M. Must, J. K. Spinler, E. M. Twiddy, and R. K. Holmes.** 2005. Analysis of truncated variants of the iron dependent transcriptional regulators from *Corynebacterium diphtheriae* and *Mycobacterium tuberculosis*. FEMS Microbiol. Lett. **243:**1–8.
42. **Patek, M., J. Nesvera, A. Guyonvarch, O. Reyes, and G. Leblon.** 2003. Promoters of *Corynebacterium glutamicum*. J. Biotechnol. **104:**311–323.
43. **Qian, Y., J. H. Lee, and R. K. Holmes.** 2002. Identification of a DtxR-regulated operon that is essential for siderophore-dependent iron uptake in *Corynebacterium diphtheriae*. J. Bacteriol. **184:**4846–4856.
44. **Qiu, X., E. Pohl, R. K. Holmes, and W. G. Hol.** 1996. High-resolution structure of the diphtheria toxin repressor complexed with cobalt and manganese reveals an SH3-like third domain and suggests a possible role of phosphate as co-corepressor. Biochemistry **35:**12292–12302.
45. **Qiu, X., C. L. Verlinde, S. Zhang, M. P. Schmitt, R. K. Holmes, and W. G. Hol.** 1995. Three-dimensional structure of the diphtheria toxin repressor in complex with divalent cation co-repressors. Structure **3:**87–100.
46. **Rodriguez, G. M., B. Gold, M. Gomez, O. Dussurget, and I. Smith.** 1999. Identification and characterization of two divergently transcribed iron regulated genes in *Mycobacterium tuberculosis*. Tuber. Lung Dis. **79:**287–298.
47. **Rodriguez, G. M., M. I. Voskuil, B. Gold, G. K. Schoolnik, and I. Smith.** 2002. *ideR*, an essential gene in *Mycobacterium tuberculosis*: role of IdeR in iron-dependent gene expression, iron metabolism, and oxidative stress response. Infect. Immun. **70:**3371–3381.
48. **Schafer, A., J. Kalinowski, and A. Puhler.** 1994. Increased fertility of *Corynebacterium glutamicum* recipients in intergeneric matings with *Escherichia coli* after stress exposure. Appl. Environ. Microbiol. **60:**756–759.
49. **Schiering, N., X. Tao, H. Zeng, J. R. Murphy, G. A. Petsko, and D. Ringe.** 1995. Structures of the apo- and the metal ion-activated forms of the diphtheria tox repressor from *Corynebacterium diphtheriae*. Proc. Natl. Acad. Sci. USA **92:**9843–9850.
50. **Schmitt, M. P.** 1997. Transcription of the *Corynebacterium diphtheriae hmuO* gene is regulated by iron and heme. Infect. Immun. **65:**4634–4641.
51. **Schmitt, M. P., and R. K. Holmes.** 1993. Analysis of diphtheria toxin repressor-operator interactions and characterization of a mutant repressor with decreased binding activity for divalent metals. Mol. Microbiol. **9:**173–181.
52. **Schmitt, M. P., and R. K. Holmes.** 1991. Characterization of a defective diphtheria toxin repressor (*dtxR*) allele and analysis of *dtxR* transcription in wild-type and mutant strains of *Corynebacterium diphtheriae*. Infect. Immun. **59:**3903–3908.

53. **Schmitt, M. P., and R. K. Holmes.** 1994. Cloning, sequence, and footprint analysis of two promoter/operators from *Corynebacterium diphtheriae* that are regulated by the diphtheria toxin repressor (DtxR) and iron. J. Bacteriol. **176:**1141–1149.
54. **Schmitt, M. P., and R. K. Holmes.** 1991. Iron-dependent regulation of diphtheria toxin and siderophore expression by the cloned *Corynebacterium diphtheriae* repressor gene *dtxR* in *C. diphtheriae* C7 strains. Infect. Immun. **59:**1899–1904.
55. **Schmitt, M. P., M. Predich, L. Doukhan, I. Smith, and R. K. Holmes.** 1995. Characterization of an iron-dependent regulatory protein (IdeR) of *Mycobacterium tuberculosis* as a functional homolog of the diphtheria toxin repressor (DtxR) from *Corynebacterium diphtheriae*. Infect. Immun. **63:**4284–4289.
56. **Schmitt, M. P., B. G. Talley, and R. K. Holmes.** 1997. Characterization of lipoprotein IRP1 from *Corynebacterium diphtheriae*, which is regulated by the diphtheria toxin repressor (DtxR) and iron. Infect. Immun. **65:**5364–5367.
57. **Serwold-Davis, T. M., and N. B. Groman.** 1986. Mapping and cloning of *Corynebacterium diphtheriae* plasmid pNG2 and characterization of its relatedness to plasmids from skin coryneforms. Antimicrob. Agents Chemother. **30:**69–72.
58. **Simon, R., U. Priefer, and A. Puhler.** 1983. A broad host range mobilization system for in vivo genetic engineering—transposon mutagenesis in Gram-negative bacteria. Bio/Technology **1:**784–791.
59. **Tao, X., J. Boyd, and J. R. Murphy.** 1992. Specific binding of the diphtheria tox regulatory element DtxR to the tox operator requires divalent heavy metal ions and a 9-base-pair interrupted palindromic sequence. Proc. Natl. Acad. Sci. USA **89:**5897–5901.
60. **Tao, X., and J. R. Murphy.** 1992. Binding of the metalloregulatory protein DtxR to the diphtheria tox operator requires a divalent heavy metal ion and protects the palindromic sequence from DNase I digestion. J. Biol. Chem. **267:**21761–21764.
61. **Ton-That, H., and O. Schneewind.** 2003. Assembly of pili on the surface of *Corynebacterium diphtheriae*. Mol. Microbiol. **50:**1429–1438.
62. **Unniraman, S., M. Chatterji, and V. Nagaraja.** 2002. DNA gyrase genes in *Mycobacterium tuberculosis*: a single operon driven by multiple promoters. J. Bacteriol. **184:**5449–5456.
63. **Virji, M.** 1997. Post-translational modifications of meningococcal pili. Identification of common substituents: glycans and alpha-glycerophosphate—a review. Gene **192:**141–147.